FLEXIBLE-ELASTIC DEFORMATION MEASUREMENT OF ZnS:Cu^{2+} MECHANOLUMINESCENT FILM USING VISUAL INSPECTION AND DIGITAL IMAGE CORRELATION

Guo-Qing Gu[1,2], Gui-Zhong Xu[1,2], Feng Shen[3], Peng Zhou[4], Hou-Chao Sun[1], Jia-Xing Weng[5]

1) Yancheng Institute of Technology, School of Civil Engineering, Yancheng, 224051, China
　(gqgu@ycit.edu.cn, ✉ guizhongxu@163.com, 442013120@qq.com)

2) Coastal City Low Carbon Construction Engineering Technology Research Center, Yancheng 224056, China

3) Jiangsu Fiber Composite Company Ltd., Jianhu, Yancheng 224700, China (alex@jsfiberwell.com)

4) Yancheng Institute of Supervision & Inspection on Product Quality, Yancheng 224056, China (326392969@qq.com)

5) Jiangsu Water Source Company Ltd. of the Eastern Route of the South-to-North Water Diversion Project,
　Nanjing 210000, China (wengjiaxingseu@163.com)

Abstract

ZnS-based mechanoluminescent film has been widely used in the fields of stress visualization and stress sensing, due to its high brightness and repeatable stable luminescent characteristics. To evaluate the flexible-elastic deformation performance of ZnS-based mechanoluminescent film, both visual inspection and *digital image correlation* (DIC) are, respectively, employed for measuring the ZnS-based mechanoluminescent film. ZnS:Cu^{2+} mechanoluminescent powders are first mixed with *polydimethylsiloxane* (PDMS) matrix to produce ZnS:Cu^{2+}–PDMS mechanoluminescent film. Then, two measurement experiments are, respectively, conducted to investigate the mechanical response and the flexible-elastic deformation performance of the prepared ZnS:Cu^{2+}–PDMS mechanoluminescent film. On one hand, the mechanical response performance of the ZnS:Cu^{2+}–PDMS mechanoluminescent film is validated by visual monitoring of composite concrete fracture processes. On the other hand, the prepared ZnS:Cu^{2+}–PDMS mechanoluminescent film is also measured by DIC to obtain its full-field deformations and strains information. The flexible-elastic deformation performance of the ZnS:Cu^{2+}–PDMS mechanoluminescent film is well demonstrated by the DIC measured results.

Keywords: ZnS:Cu^{2+}–PDMS mechanoluminescent film, flexible-elastic deformation performance, visual inspection, digital image correlation.

1. Introduction

As massive civil infrastructures enter service, new and old damages develop and accumulate continuously, leading to deterioration of material properties and safety incidents [1, 2]. For this reason, reliable *structural health monitoring* (SHM) is essential for assessing the service status of infrastructure systems and formulating operation and maintenance strategies. With the increasing research on mechanoluminescent materials, the engineering community is actively exploring the use of stress/strain sensors based on the mechanoluminescence phenomenon for SHM of civil infrastructure [3–7]. It is well known that mechanoluminescence is a force-induced luminescence phenomenon that occurs when a material is subjected to external mechanical stimulation. Depending on the form of stress excitation, mechanoluminescence can be classified as frictional mechanoluminescence, fracture mechanoluminescence, elastic mechanoluminescence and plastic mechanoluminescence [8]. Among these, sensors based on elastic mechanoluminescence can visualize structural stress distribution and have a huge potential to detect structural deformation, fatigue damage and fracture breakage.

Xu *et al.* were the first to compound SrAl2O4:Eu^{2+} with epoxy resin to prepare elastic mechanoluminescent films, which were successfully used for structural damage monitoring [9]. This application discovery offered a completely new idea for engineering application of mechanoluminescent materials. Subsequently, many new mechanoluminescent materials with superior properties have been explored and developed, including aluminates, silicates, phosphates, titanates, sulphur compounds, oxy-sulphides, fluorides, *etc*. [10–12]. Among them, ZnS-based mechanoluminescent materials are the most studied and promising class of mechanoluminescent materials, including ZnS:Mn^{2+} and ZnS:Cu^{2+} [13, 14]. In order to use ZnS-based mechanoluminescent materials for stress visualization and monitoring of engineering structures and mechanical equipment, some studies have reported on the preparation of ZnS:Mn^{2+}, ZnS:Cu^{2+} or other mechanoluminescent materials by compounding them with some polymer resins, *e.g.*, epoxy resin, *polyvinylidene fluoride* (PVDF), *polydimethylsiloxane* (PDMS), *etc.*, to form elastic mechanoluminescent films. For example, Fontenot *et al.* systematically investigated the mechanical, spectral, and luminescence properties of ZnS:Mn^{2+}-PDMS mechanoluminescent films [15]. Krishnan *et al.* characterized the light emission from ZnS:Cu^{2+}–PDMS mechanoluminescent films during elastic loading for application in dynamic SHM [16]. Zhu *et al.* prepared ZnS:Mn^{2+}-PVDF flexible mechanoluminescent films with a composite and analysed their luminescent properties [17]. Zhang *et al.* investigated the impact optical response of ZnS:Cu^{2+}/water glass mechanoluminescent films by light air cannon impact experiments [18]. Wang *et al.* used ZnS:Mn^{2+}-PVDF-ZnS:Mn^{2+} multilayer structure to prepare flexible mechanoluminescent films and revealed the enhancement effect of the applied electric field on the luminescent properties of the films [19]. Han *et al.* prepared ZnS:Mn^{2+}-PDMS mechanoluminescent thin films through high-temperature solid-phase synthesis and introduced them to the study of oral material applications [20]. Although the studies above provide an important basis for the application of ZnS-based mechanoluminescent films for stress visualization and monitoring, there is a lack of analytical studies on the mechanical properties of ZnS-based mechanoluminescent films, especially on the structural mechanical response properties.

In this paper, a ZnS:Cu^{2+}–PDMS mechanoluminescent film was prepared by a combination of ZnS:Cu^{2+} mechanoluminescent material and PDMS matrix. Both visual inspection and *digital image correlation* (DIC) method were used to characterize the performance of the ZnS:Cu^{2+}–PDMS mechanoluminescent film. Visual monitoring of the tensile fracture process of concrete

specimen was conducted to verify the mechanical response property of the $ZnS:Cu^{2+}$–PDMS mechanoluminescent film. Moreover, DIC was employed to measure the axial tensile mechanical properties of $ZnS:Cu^{2+}$–PDMS mechanoluminescent film.

2. Materials and Measurement Methods

2.1. Mechanoluminescent Film Sample

A certain mass of the commercial mechanoluminescent powder $ZnS:Cu^{2+}$ (Shanghai Keyan Phosphor Technology Co., Ltd) and PDMS (Dow Corning (China) Silicone Co., Ltd) was weighed, and mixed in a 1:1 mass ratio to form a solution. The PDMS is commonly known as silicone rubber, and its curing agent ratio is usually between 5:1 to 10:1. The mixed solution was stirred well with a magnetic stirrer, and the flowing method was used to make it fully and evenly distributed on a $100 \times 100 \times 1$ mm :glassware, with a scraper to further control the flowing liquid. Besides, the thickness of the cast liquid was controlled by a squeegee. Then, the cast liquid was placed in a vacuum drying oven, and vacuumed to -0.02 MPa, and removed after 5 min to reduce the cast liquid bubbles. As the cast liquid mixture is a medium viscosity liquid before curing, it becomes a tough elastomer only after curing. The glassware containing the cast mixture was placed in an oven and cured at $70°C$ for 90 min. After curing, the gel was carefully removed from the glassware and a sample of the $ZnS:Cu^{2+}$–PDMS mechanoluminescent film was finally obtained.

$ZnS:Cu^{2+}$–PDMS mechanoluminescent film specimen of $80 \times 30 \times 1$ mm: was cut out from the $100 \times 100 \times 1$ mm sample prepared above using a hobby knife, as shown in Fig. 1a. In order to test the mechanoluminescence properties of the $ZnS:Cu^{2+}$–PDMS mechanoluminescent film, the specimen was repeatedly stretched with a simple self-made tension testing machine in a dark room environment to apply mechanical stress stimulation, and the luminescence effect of the film was real-time photographed with an E750D Canon camera. Fig. 1b shows one instant picture during the whole light emission procedure. It can be found that the $ZnS:Cu^{2+}$–PDMS mechanoluminescent

a) Sample of $ZnS:Cu^{2+}$–PDMS film.   b) Picture of lighted $ZnS:Cu^{2+}$–PDMS film.

Fig. 1. Mechanoluminescent film sample preparation.

film emitted a strong blue-green light in a dark room environment, indicating that the ZnS:Cu^{2+}–PDMS mechanoluminescent film specimen was successfully prepared.

Meanwhile, a photomultiplier tube (PMM01, THORLABS) was also adopted here to detect the photo-current intensity when the ZnS:Cu^{2+}–PDMS mechanoluminescent film specimen made a continuous light emission. The satisfactory linear curve relation between the photo-current intensity and the tensile stress is well depicted in Fig. 2. Fig. 2a presents a linear least square fit curve, and Fig. 2b shows a residual diagram accordingly. In result, the linear least square fitted function can be expressed as $y = 0.0103 \cdot x + 0.004773$, the *root mean squared error* (RMSE) equals 0.00306, the sum of squares due to error (SSE) equals 8.428×10^{-5}, and the coefficient of determination (R-square) equals 0.9928. It can be seen from the error statistical parameters above that there is a better linear relation between the mechanoluminescent intensity and the induced tensile stress. That is to say, the larger induced stress is applied to the ZnS:Cu^{2+}–PDMS mechanoluminescent film specimen, the stronger is its light emission, and the greater the photo-current intensity acquisition. Therefore, it can be indicated that the prepared ZnS:Cu^{2+}–PDMS mechanoluminescent film indeed exhibits an outstanding elastic mechanoluminescence capability.

a) Linear least square fit curve.
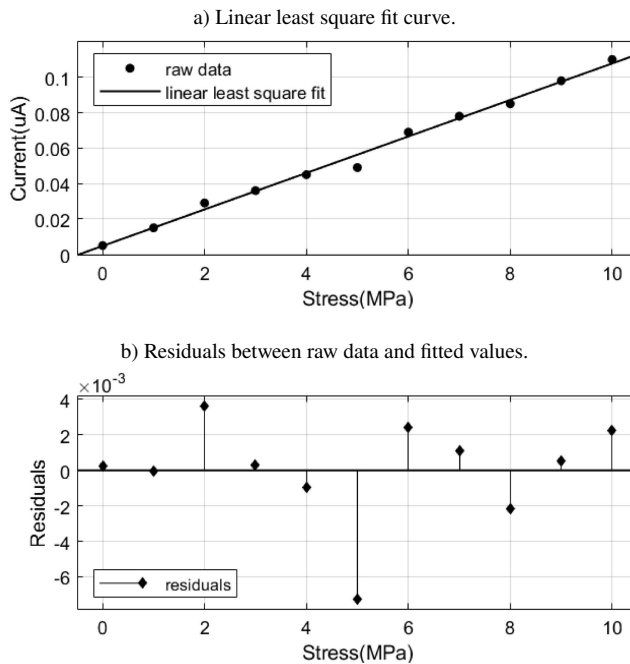

b) Residuals between raw data and fitted values.

Fig. 2. Linear relation between photo-current intensity and tensile stress of ZnS:Cu2+-PDMS film.

2.2. Principle of the Two-Dimensional Digital Image Correlation Method

In order to further investigate the mechanical properties of the prepared ZnS:Cu^{2+}–PDMS mechanoluminescent film, and especially its elastic mechanical properties, tensile tests will be carried out on the ZnS:Cu^{2+}–PDMS mechanoluminescent film specimens using the DIC method.

As is well known, DIC possesses the advantages of simple optical path, good environmental adaptability, wide measurement range and high degree of automation, and has been widely used in full-field non-contact testing of mechanical properties of materials [21, 22].

The *two-dimensional* (2D) DIC method is mainly used to obtain the full-field deformation and strain information of the surface of the object under test through the mutual correlation of the speckle images before and after deformation. Fig. 3 shows the principle of the 2D DIC method. In the speckle image before deformation, the $N \times N$ rectangular image sub-region with the point (x, y) is taken as the centre. to determine the target speckle image after the deformation, a certain search method is used and according to a certain correlation function, a correlation operation is carried out to find the $N \times N$ target rectangular area with the point (x', y') as the centre that has the maximum correlation coefficient with the rectangular sub-region taken before the deformation. The pixel shifts of the sub-regions of the image are thus determined.
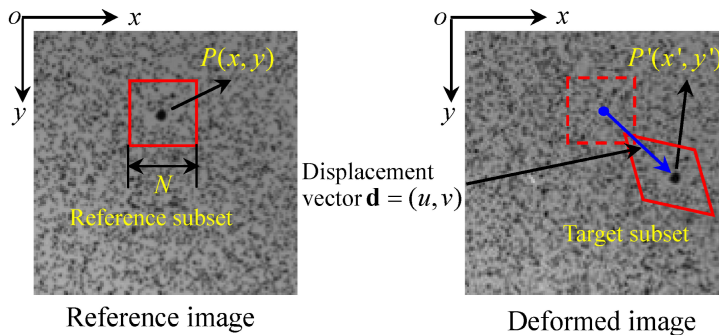

Fig. 3. Principle of the 2D digital image correlation method.

A standardized covariance correlation function with high resistance to interference was used to evaluate the similarity of image sub-regions [23, 24].

$$C = \frac{\sum\sum[(f - \langle f \rangle) \cdot (g - \langle g \rangle)]}{\left[\sum\sum(f - \langle f \rangle)^2 \cdot \sum\sum(g - \langle g \rangle)^2\right]^{\frac{1}{2}}} \cdot \tag{1}$$

The range of values of C is [–1, 1], with correlation coefficient equal to 1 indicating perfect correlation, while the correlation coefficient equal to 0 indicates no correlation at all. Here, $f = f(x, y)$, $g = g(x + u, y + v)$ are the grey scale values of the speckle image centred on the source and target points respectively; u, v are their horizontal and vertical displacement values respectively, and $\langle f \rangle$ and $\langle g \rangle$ are their systematic average grey scale values respectively.

3. Experiments and Results

3.1. Visual Inspection Experiment

To investigate the structural mechanical response of the prepared $ZnS:Cu^{2+}$–PDMS mechano-luminescent film, a visual inspection experiment was first conducted. The prepared film was pasted onto the surface of concrete specimen to visually inspect the concrete fracture cracks. Its real-time

response to concrete stress changes was recorded by a camera to achieve visual monitoring of the concrete fracture process. Concrete test blocks of $100 \times 100 \times 200$ mm were cast with two different strength classes, C50 and ECC80, respectively. After curing, the C50 and ECC80 concrete specimens were directly glued together using epoxy resin to form a composite concrete specimen. The composite concrete specimen was then polished. The surface of the prepared ZnS:Cu^{2+}–PDMS mechanoluminescent film was treated with YH–840A silicone. After 10 minutes, the treated film was then coated with YH–840B glue to firmly adhere to the surface of the composite concrete test block.

As shown in Fig. 4, the composite concrete specimen with the ZnS:Cu^{2+}–PDMS mechanoluminescent film was clamped and fixed on a tensile testing machine (WDW–100E, Jinan Shijin Testing Machine Group Co., Ltd.) to carry out a study on the application of tensile fracture monitoring of composite concrete specimen. An E750D Canon camera was used to record the tensile process of the composite concrete specimens. Before the tensile testing, the maximum stress level was initially set to 2 MPa. Meanwhile, during the testing, a portable optical fibre spectrometer (XS11639, Shanghai Oceanhood Opto-electronics Tech. Co.) was also used for recording the real-time spectrum of the film adhered to the surface of the composite concrete test block. The spectra were captured by the spectrometer every 5 seconds. When the tensile stress applied to the composite concrete test block reached 1.89 MPa, the composite concrete specimen fractured and separated at the epoxy cement joint. Fig. 5 shows the dynamic spectrum diagram. The spectrum intensity obviously increases with the change of the loading time. At the time of 55 s, the ZnS:Cu^{2+}–PDMS mechanoluminescent film emitted a bright blue-green light due to the impact on its fracture on it, as shown in Fig. 5. The emitted light intensity of the ZnS:Cu^{2+}–PDMS mechanoluminescent film gradually raised with the tensile stress increasing, as shown in the enlarged illustration in Fig. 5. This indicates that the ZnS:Cu^{2+}–PDMS mechanoluminescent film is quite sensitive to the fracture stress of composite concrete specimen and provides a rapid and repeatable response, which can better visualize the stress in the fracture process of composite concrete specimen.
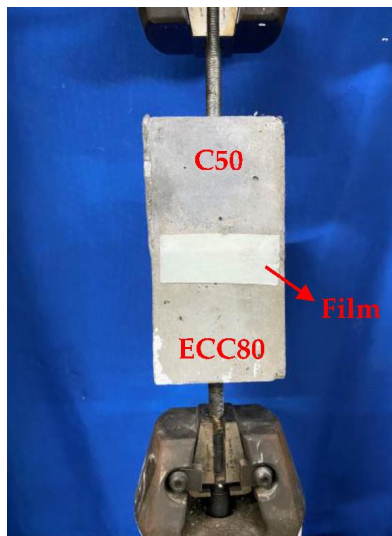

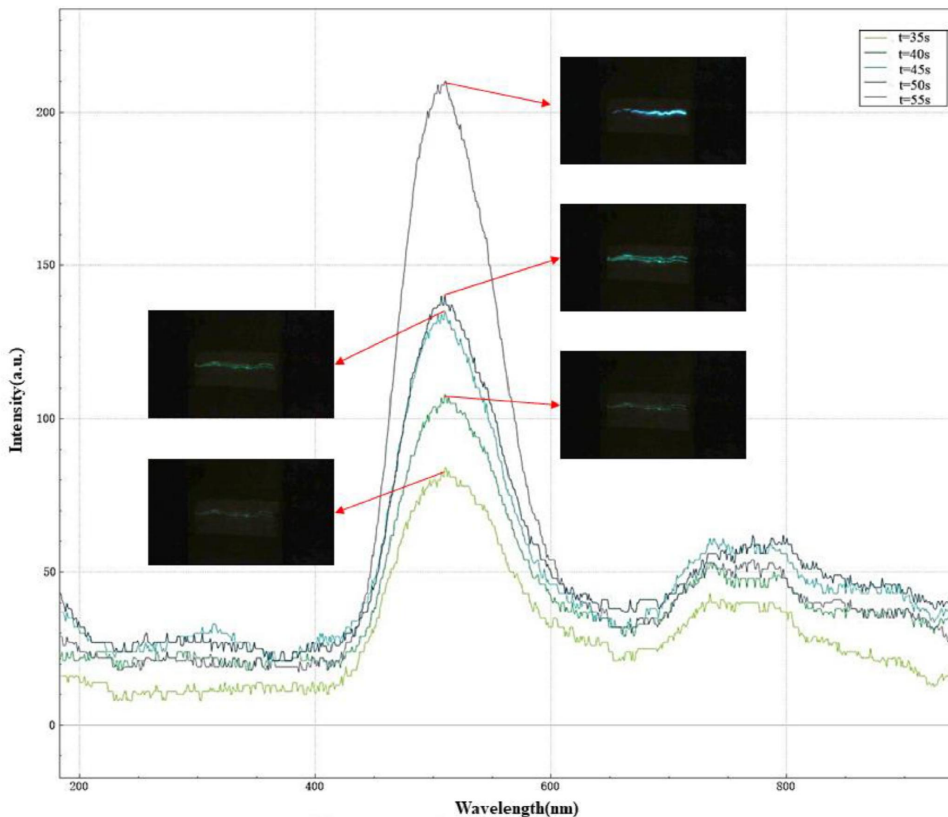Fig. 4. Visual inspection tensile testing of the concrete fracture process.

Fig. 5. Dynamic spectrum corresponding to the visualization monitoring of the concrete fracture process.

3.2. DIC Measurement Experiment

Before DIC measurement experiment, a random speckle pattern was first prepared on the surface of the ZnS:Cu^{2+}–PDMS mechanoluminescent film specimen using the paint spray method, as shown in the enlarged illustration in Fig. 6. Then, a simple system for DIC testing was constructed as shown in Fig. 6 for axial tensile testing. The ZnS:Cu^{2+}–PDMS mechanoluminescent film specimen was fixed with the calliper device of the tensile testing machine (ZQ99L, Dongguan Zhiqu Instrument Co., Ltd.), and the axial tensile stress was applied at a rate of 4 mm/min. The illumination source was switched on and the optical axis of the camera lens (HF16SA-1, FUJINON) was adjusted to be perpendicular to the film specimen. A high-definition industrial COMS camera (GS3-U3-51S5M-C, PGR) was used for acquisition of speckle images of the film specimen. Fig. 7 presents an instantaneous speckle image captured by the COMS camera, which will be then analysed by the DIC algorithm. It was an 8-bit grayscale image, and had a width of 2448 pixel and a height of 2048 pixel. The DIC software, Ncorr, an open source 2D DIC MATLAB program [25], was herein used to correlate the speckle images before and after the deformation illustrated in Fig. 7 to obtain the full-field displacement and strain distributions on the surface of the ZnS:Cu^{2+}–PDMS mechanoluminescent film specimen. The dimension of the selected *region of interest* (ROI) of Fig. 7 was 500×1000 pixels, which was located in the centre region of the specimen.
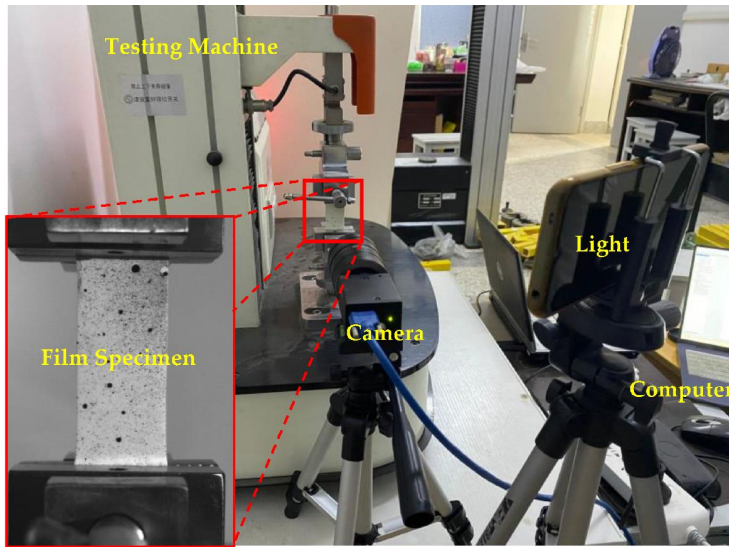
Fig. 6. DIC tensile testing of ZnS:Cu^{2+}–PDMS mechanoluminescent film.

Fig. 7. DIC tensile test of ZnS:Cu^{2+}–PDMS mechanoluminescent film.

Fig. 8 shows the x- and y-directional u- and v-field displacements of the ZnS:Cu^{2+}–PDMS mechanoluminescent film specimen under an axial tensile stress of 2 MPa. It is obvious to find that the ZnS:Cu^{2+}–PDMS mechanoluminescent film exhibits good elastic deformation under axial tensile stress. This completely confirms its good flexibility and makes it possible to apply the elastic mechanoluminescent film for structural stress-strain sensing. As shown in Fig. 8a, the ZnS:Cu^{2+}–PDMS mechanoluminescent film undergoes shrinkage elastic deformation from the sides to the middle along the x-direction under axial tensile loading. As shown in Fig. 8b, under axial tensile loading, it undergoes tensile elastic deformation along the y-direction, which is the dominant deformation of the specimen under axial tensile stress.
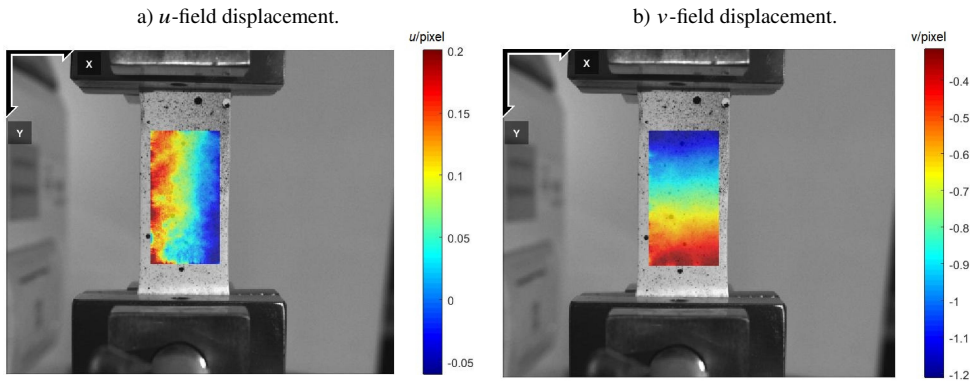
a) *u*-field displacement.

b) *v*-field displacement.

Fig. 8. DIC displacements of ZnS:Cu^{2+}–PDMS mechanoluminescent film.

Fig. 9 shows the strain distributions of the ZnS:Cu^{2+}–PDMS mechanoluminescent film specimen in the $\mathcal{E}_{xx}$, $\mathcal{E}_{yy}$, and $\mathcal{E}_{xy}$ fields under an axial tensile stress of 2 MPa. The $\mathcal{E}_{xx}$ and $\mathcal{E}_{yy}$ represent the normal strains along *x*-direction and *y*-direction, respectively, whereas $\mathcal{E}_{xy}$ denotes the shear strain that is determined with the angle change between *x*-direction and *y*-direction. As
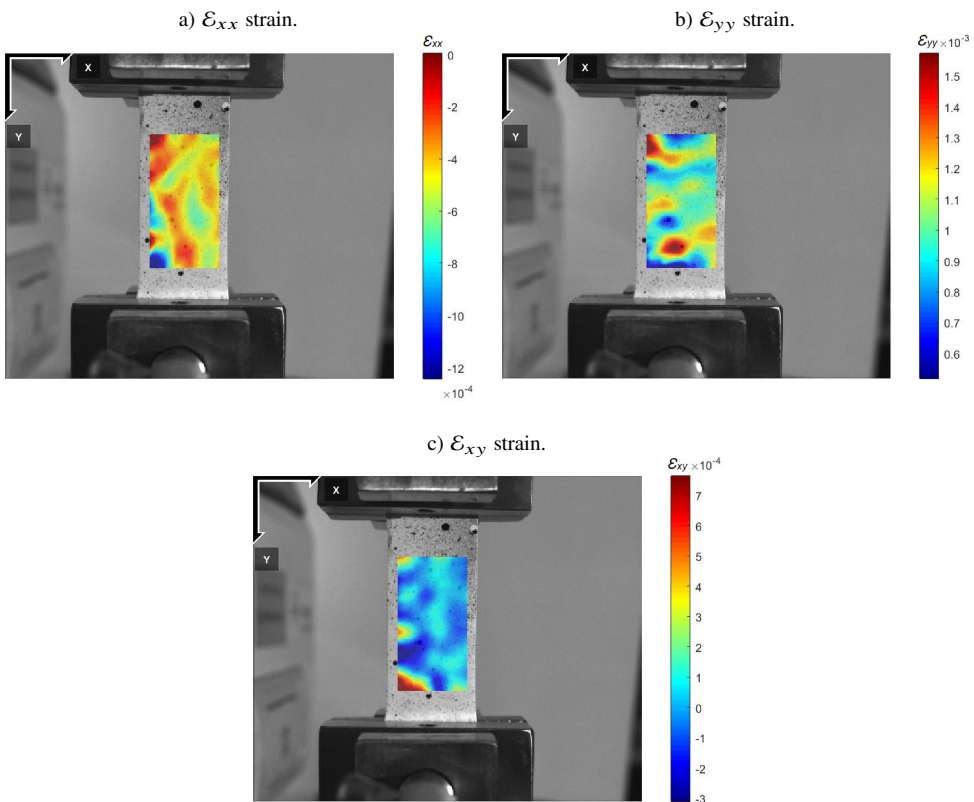
a) $\mathcal{E}_{xx}$ strain.

b) $\mathcal{E}_{yy}$ strain.

c) $\mathcal{E}_{xy}$ strain.

Fig. 9. DIC strains of ZnS:Cu^{2+}–PDMS mechanoluminescent film.

can be seen from Fig. 9, the strain distribution on the surface of the ZnS:Cu^{2+}–PDMS stress-emitting film specimen shows non-uniform characteristics, which is directly related to the fact that the ZnS:Cu^{2+} mechanoluminescent powder particles in the ZnS:Cu^{2+}–PDMS mechanoluminescent film are not fully uniformly stirred with the PDMS matrix. Inadequate mixing with the PDMS matrix will make the powder particles in the cured film unevenly distributed resulting in localized agglomeration of powder particles, thus making the film stretching occur as localized strain concentration phenomenon shown in Fig. 9b. In addition, uneven strain distribution may also be associated with inconsistent film thickness. When the film thickness was controlled using a squeegee, the ZnS:Cu^{2+}–PDMS mechanoluminescent film is a medium viscosity liquid until it is fully cured. The liquid inevitably spreads around as it cures, resulting in reduced thickness at the edges of the formed film, triggering slightly lower strains at the edges of the film.

4. Conclusions

In this paper, the ZnS:Cu^{2+} mechanoluminescent material was used to mix with PDMS matrix to prepare the ZnS:Cu^{2+}–PDMS mechanoluminescent film. In order to comprehensively evaluate the mechanical performances of the film, both visual inspection and DIC test experiments were carried out.

For visual inspection, the ZnS:Cu^{2+}–PDMS mechanoluminescent film provided a sensitive response to fracture cracks in real time when a composite concrete specimen was fractured in tension at the cemented joint. Furthermore, the luminescence of the ZnS:Cu^{2+}–PDMS mechanoluminescent film gradually decreased with stress decay. This demonstrates that the ZnS:Cu^{2+}–PDMS mechanoluminescent film has good structural mechanical response properties and can be used for stress-strain sensing and visualization of engineering structures.

For DIC test, the information of surface deformation and strain distributions of ZnS:Cu^{2+}–PDMS mechanoluminescent film were obtained with the full-field non-destructive DIC method. Additionally, the DIC test results fully indicate that the ZnS:Cu^{2+}–PDMS mechanoluminescent film exhibits quite good flexible-elastic deformation performance.

References

[1] Nsengiyumva, W., Zhong, S. C., Lin, J. W., Zhang, Q. K., Zhong, J. F., & Huang, Y. X. (2021). Advances, limitations and prospects of nondestructive testing and evaluation of thick composites and sandwich structures: A state-of-art review. *Composite Structures*, 256, 112951. https://doi.org/10.1016/j.compstruct.2020.112951

[2] Sun, H., Wang, T., Lin, D. W., Wang, Y. S., & Qing, X. L. (2020). An eddy current-based structural health monitoring technique for tracking bolt cracking. *Sensors*, 20, 6843. https://doi.org/10.3390/s20236843

[3] Lyu, L., Ohnuma, Y., Shigemoto, Y., Hanada, T., Fukada, T., Akiyama, H., Tersaki, N., & Horiuchi, S. (2020). Toughness and durability of interfaces in dissimilar adhesive joints of aluminum and carbon-fiber-reinforced thermoplastics. *Langmuir*, 36(46), 14046–14057. https://doi.org/10.1021/acs.langmuir.0c02628

[4] Jha, P., & Khare, A. (2020). SrAl2O4:Eu, Dy mechanoluminescent flexible film for impact sensors. *Journal of Alloys and Compounds*, *847*, 156428. https://doi.org/10.1016/j.jallcom.2020.156428

[5] Zhou, J. Y., Gu, Y., Lu, J. Y., Xu, L. D., Zhang, J. C., Wang, D, & Wang, W. X. (2020). An ultrastrong non-pre-irradiation and self-recoverable mechanoluminescent elastomer. *Chemical Engineering Journal*, *390*, 124473. https://doi.org/10.1016/j.cej.2020.124473

[6] Makris, B., Hille, F., Thiele, M., Kirschberger, D., & Sowietzki, D. (2018). Crack luminescence as an innovative method for detection of fatigue damage. *Journal of Sensors and Sensor Systems*, 7, 259–266. https://doi.org/10.5194/jsss-7-259-2018

[7] Timilsina, S., Bashnet, R., Kim, S. H., Lee, K. H., & Kim, J. S. (2017). A life-time reproducible mechano-luminescent paint for the visualization of crack propagation mechanisms in concrete structures. *International Journal of Fatigue*, *101*, 75–79. https://doi.org/10.1016/j.ijfatigue.2017.03.011

[8] Yuan, Y., Yuan, W., Chen, Y. L. (2016). Recent advances in mechanoluminescent polymers. *Science China Materials*, *59*(6), 507–520. https://doi.org/10.1007/s40843-016-5060-7

[9] Xu, C. N., Watanabe, T., Akiyama, M., & Zheng, X. G. (1999). Direct view of stress distribution in solid by mechanoluminescence. *Applied Physics Letters*, *74*(17), 2414–2416. https://doi.org/10.1063/1.123865

[10] Jha, P., & Chandra, B. P. (2014). Survey of the literature on mechanoluminescence from 1605 to 2013. *Luminescence*, *29*(8), 977–993. https://doi.org/10.1002/bio.2647

[11] Chandra, B. P., Chandra, V. K., & Jha, P. (2015). Mechanoluminescence of coloured alkali halide crystals. *Defect Diff. Forum*, *361*, 121–176. https://doi.org/10.4028/www.scientific.net/DDF.361.121

[12] Chandra, B. P., Chandra, V. K., & Jha, P. (2015). Elastico-mechanoluminescence and crystal-structure relationships in persistent luminescent materials and II-VI semiconductor phosphors. *Physica B: Condensed Matter*, 463, 62–67. https://doi.org/10.1016/j.physb.2015.01.030

[13] Shin, S. W., Oh, J. P., Hong, C. W., Kim, E. M., Woo, J. J., Heo, G. S., & Kim, J. H. (2016). Origin of mechanoluminescence from Cu-doped ZnS particles embedded in an elastomer film and its application in flexible electro-mechanoluminescent lighting devices. *ACS Applied Materials & Interfaces*, *8*(2), 1098–1103. https://doi.org/10.1021/acsami.5b07594

[14] Zhuang, Y. X., & Xie, R. J. (2021). Mechanoluminescence of rebrightening the prospects of stress sensing: a review. *Advanced Materials*, *33*, 2005925. https://doi.org/10.1002/adma.202005925

[15] Fontenot, R. S., Allison, S. W., Lynch, K. J., Hollerman, W. A., & Sabri, F. (2016). Mechanical, spectral, and luminescence properties of ZnS:Mn doped PDMS. *Journal of Luminescence*, *170*, 194–199. https://doi.org/10.1016/j.jlumin.2015.10.047

[16] Krishnan, S., Van der Walt, H., Venkatesh, V., Sundaresan, V. B. (2017). Dynamic characterization of elastico-mechanoluminescence towards structural health monitoring. *Journal of Intelligent Material Systems and Structures*, *28*(17), 1-7. https://doi.org/10.1177/1045389X17689939

[17] Zhu, J. G., Chen, C. F., Zhang, R. F. (2021). Electroprinting of MWCNT-assisted PVDF thin films with enhanced electrical properties. *Applied Surface Science Advances*, *5*, 100115. https://doi.org/10.1016/j.apsadv.2021.100115

[18] Zhang, G. D., Zhao, Y. L., Sun, J., Wei, X. Y. (2022). Optical response and application of mechano-luminescent film of ZnS:Cu under impact pressure. *Chinese Journal of High Pressure Physics*, *36*(2), 021301. https://doi.org/10.11858/gywlxb.20210899 (in Chinese)

[19] Wang, F. L., Wang, F. L., Wang, X. D., Weng, S. C., Jiang, J. F., Liu, Q. L., Hao, X. T., Han, L., Wang, J. J., Pan, C. F., Liu, H., & Sang, Y. H. (2019). Mechanoluminescence enhancement of ZnS:Cu, Mn with piezotronic effect induced trap-depth reduction originated from PVDF ferroelectric film. *Nano Energy*, *63*, 103861. https://doi.org/10.1016/j.nanoen.2019.103861

[20] Han, Y., Bai, Y. Q., Bian, J. L., Guo, X. P., Liu, B., & Wang, Z. F. (2021). Polydimethylsiloxane-based mechanoluminescent occlusal splint with the visualization of occlusal force. *ACS Applied Polymer Materials*, *3*(10), 5180–5187. https://doi.org/10.1021/acsapm.1c00917

[21] Pan, B. (2018). Digital image correlation for surface deformation measurement: historical developments, recent advances and future goals. *Measurement Science and Technology*, *29*, 081001. https://doi.org/10.1088/1361-6501/aac55b

[22] Gao, H. L., Lin, Z. Y., Huang, X. W., Shang, H. B., & Zhan, J. S. (2022). In situ measurement of cyclic plastic zone and internal strain response of Q & P steel near fatigue crack tip region based on micro-DIC. *Materials*, 15(17), 6114. https://doi.org/10.3390/ma15176114

[23] Gu, G., Xu, G. Z., & Xu, B. (2018). Synchronous measurement of out-of-plane displacement and slopes by triple-optical-path digital speckle pattern interferometry. *Metrology and Measurement Systems*, *25*(1), 3–14. https://doi.org/10.24425/118159

[24] Qi, J. K., Xu, M. Q., Zhang, W. L., Liu, Y. B., & Dai, X. J. (2022). Defect detection of pipeline inner surface based on coaxial digital image correlation with hypercentric lens. *Materials*, *15*(21), 7543. https://doi.org/10.3390/ma15217543

[25] Blaber, J., Adair, B., & Antoniou, A. (2015). Ncorr: Open-Source 2D Digital Image Correlation Matlab Software. *Experimental Mechanics*, *55*, 1105–1122. https://doi.org/10.1007/s11340-015-0009-1

Guoqing Gu received the Ph.D. degree from Nanjing University of Aeronautics & Astronautics, China, in 2013. He is currently an Associate Professor of the School of Civil Engineering of Yancheng Institute of Technology. His research activity focuses on experimental mechanics.

Feng Shen received the B.Sc. degree from Nanjing University of Science and Technology, China, in 1997. He is currently the Chairman and General Manager of the Jiangsu Fiber company. His research activity focuses on intelligent FRP composite structures.

Guizhong Xu received the Ph.D. degree from Hohai University, China, in 2013. He is currently a Professor of the School of Civil Engineering of Yancheng Institute of Technology. His research activity focuses on intelligent and ecological geotechnical engineering.

Peng Zhou received the B.Sc. degree from Yancheng Institute of Technology, China, in 2008. He is currently an Assistant Engineer of Yancheng Institute of Supervision & Inspection on Product Quality. His main research interest is mechanical testing.

Houchao Sun received the Ph.D. degree from Nanjing Forestry University, China, in 2015. He is currently an Associate Professor of the School of Civil Engineering of Yancheng Institute of Technology. His research activity focuses on Prefabricated Building Technology.

Jiaxing Weng received the Ph.D. degree from Southeast University, China, in 2021. He is currently a postdoc at the Jiangsu Water Source Co., Ltd. on the East Route of the South to North Water Transfer Project. His main research activity focuses on mechanical testing and digital twin technology.